

Odd-parity superconductivity in Weyl semimetals

Huazhou Wei,¹ Sung-Po Chao,^{2,3} and Vivek Aji¹

¹*Department of Physics and Astronomy, University of California, Riverside, California 92521, USA*

²*Physics Division, National Center for Theoretical Science, Hsinchu 30013, Taiwan, R.O.C.*

³*Physics Department, National Tsing Hua University, Hsinchu 30013, Taiwan, R.O.C.*

(Received 15 May 2013; revised manuscript received 16 December 2013; published 10 January 2014)

Unconventional superconducting states of matter are realized in the presence of strong spin-orbit coupling. In particular, nondegenerate bands can support odd-parity superconductivity with rich topological content. Here we study whether this is the case for Weyl semimetals. These are systems whose low-energy sector, in the absence of interactions, is described by linearly dispersing chiral fermions in three dimensions. The energy spectrum has nodes at an even number of points in the Brillouin zone. Consequently both intranodal finite momentum pairing and internodal BCS superconductivity are allowed. For local attractive interaction the finite momentum pairing state with chiral p -wave symmetry is found to be most favorable at finite chemical potential. The state is an analog of the superfluid $^3\text{He A}$ phase, with Cooper pairs having finite center-of-mass momentum. For chemical potential at the node the state is preempted by a fully gapped charge density wave. For nonlocal attraction the BCS state wins out for all values of the chemical potential.

DOI: [10.1103/PhysRevB.89.014506](https://doi.org/10.1103/PhysRevB.89.014506)

PACS number(s): 74.20.Rp, 74.20.Fg, 74.25.Jb, 74.70.-b

I. INTRODUCTION

Weyl semimetals are a class of materials whose low-energy description is in terms of linearly dispersing massless fermions in three dimensions. They occur in systems where two nondegenerate bands touch at isolated points in the Brillouin zone. In general the existence of such Weyl nodes at the chemical point is accidental,¹ but if they do exist then they are robust against perturbations that do not break translational invariance. The presence of degenerate chiral nodes separated in momentum space requires that either inversion or time-reversal symmetry be broken. There are a number of nontrivial consequences such as open Fermi surfaces for surface states, anomalous Hall effects, and other transport features.²⁻⁷ These phenomena can be traced back to the conservation of chirality at the Weyl nodes. While Weyl fermions have been studied extensively in the context of liquid ^3He , the recent proposals of realizing them in pyrochlore iridates² and topological-normal insulator (TNI) heterostructure³ has renewed interest on the subject.

Of particular interest is the nature of correlated phases they support. For chemical potential at the nodes, perfect nesting leads to possible particle-hole instabilities. For local repulsion, an excitonic ferromagnetic insulator is stabilized,⁸ while for local attractive interactions a charge density wave (CDW)⁹ is realized. Meng and Balents¹⁰ studied the nature of superconducting state obtained in systems where the superconductivity is externally induced by proximity effect. This is achieved by replacing the normal insulator by a superconductor in the topological-normal insulator (TNI) heterostructure. They find a variety of gapless and/or topological superconducting phases which may host Majorana bound states on the surface or vortex cores. Cho *et al.*¹¹ studied the intrinsic superconducting instabilities of doped Weyl semimetals within a model that has C_{4h} point-group symmetry. They find that the even-parity fully gapped finite momentum pairing state is energetically favored. The point-group symmetry imposed is not necessary for Weyl semimetals. In this work we relax this constraint and explore the possible superconducting phases.

For local attractive interactions we find the finite momentum pairing to be the ground state, while for long-range interaction a gapped BCS state is a competing phase, with details of the interaction favoring one over the other. Crucially, contrary to Cho *et al.*¹¹ we find that a “spin singlet” has no weight and that only p -wave “spin triplet” phases are allowed. The difference originates from the properties of the model under inversion. While our work also focuses on inversion symmetric systems, the difference arises from the nature of the low-energy states. In particular the inversion operator in our model for the two-component Weyl fermions is the identity whereas it is proportional to σ_z in Ref. 11. In Ref. 11 a preferred axis, z , is chosen by the crystal symmetry for all momenta and allows classification of superconducting states into singlets and triplets globally. For an effective model of the low-energy sector of some Weyl semimetals this indeed might be the correct description, but there is no *a priori* reason that this is the generic behavior. The lower symmetry in Ref. 11 allows for singlet states to have finite overlap with the states of the band, which is not possible if the full symmetry existed. For the class of Weyl semimetals studied in our paper, we generically find odd-parity superconductivities which are analogs of the $^3\text{He A}$ phase. They add to a class of spin triplet superconducting phases that display Weyl behavior.^{12,13}

The approach we take is the same as the one used to explore excitonic phases.⁸ In this regard the work is complementary to that of Cho *et al.*,¹¹ who look at mean-field decomposition in the spin basis prior to projecting to the low-energy sector. We first project to the linearly dispersing chiral basis, find the general expression for the particle-particle interactions in the second section, and then perform the mean-field analysis in the third section. To highlight the physics, we simplify to the case of two Weyl nodes with density-density interactions. There are two types of particle-particle instabilities that can arise in this case: (i) intranodal (occurring at zero momentum) and (ii) internodal (occurring at a finite fixed momentum associated with the nesting vector). The former leads to finite

momentum pairing [analogous to the Fulde-Ferrell-Larkin-Ovchinnikov (FFLO) state^{14,15}] while the latter is the zero momentum pairing BCS¹⁶ state. For local interaction, the most favorable superconducting state is the finite momentum paired odd-parity axial phase. A minimum interaction strength is required to nucleate them for chemical potential at the node which is the consequence of the vanishing density of states. We also find that it is energetically less optimal than a fully gapped CDW phase. For finite chemical potential the particle-hole nesting is lost, and the axial superconductor is realized. For nonlocal attraction a fully gapped BCS state is stabilized for all values of the chemical potential. The effect of disorder and topological excitations in these phases are discussed in Sec. IV. We summarize our results and compare it with others in the literature^{3,10,11} in the last section.

II. MODEL HAMILTONIAN

Consider a generic system with two Weyl nodes at $\vec{K}_0 = K_0\hat{x}$ (labeled R) and $-\vec{K}_0 = -K_0\hat{x}$ (labeled L) with chiralities $+1$ and -1 respectively. The Hamiltonian is

$$H_{0\pm} = \pm\hbar v \sum_{\vec{k}} \psi_{\vec{k}\alpha}^\dagger \vec{\sigma}_{\alpha\beta} \cdot (\vec{k} \mp \vec{K}_0) \psi_{\vec{k}\beta}, \quad (1)$$

where v is the Fermi velocity and $\vec{\sigma} = \{\sigma_x, \sigma_y, \sigma_z\}$ is a vector of Pauli matrices. The dispersion at each node is $\epsilon_{\vec{q}} = \pm\hbar v|\vec{q}|$ centered around $\pm\vec{K}_0$, with $\vec{q} = (\vec{k} \mp \vec{K}_0)$. Note that a rotation by π about the z axis of the spin basis for states near the L node maps our Hamiltonian to the one in Ref. 11. This changes the reflection symmetries of the model, which in turn modifies the nature of the possible superconducting states. The conduction (valence) band at the R node has its spin parallel (antiparallel) to \vec{q} , while the opposite is true at the L node. The general particle-particle interaction, in momentum space, takes the form

$$V = \sum_{\sigma, \sigma'} \sum_{\vec{k}, \vec{k}', \vec{q}} V(\vec{q}) \psi_{\vec{k}+\vec{q}, \sigma}^\dagger \psi_{\vec{k}', \sigma'} \psi_{\vec{k}-\vec{q}, \sigma}^\dagger \psi_{\vec{k}', \sigma'}. \quad (2)$$

Since the Weyl physics is the low-energy description of a more general theory, we enforce an upper cutoff in the momentum integrals (up to an energy Λ) around the Weyl point.

To perform mean-field analysis with attractive interaction on the particle-particle channels, we rewrite the interaction in the basis of the noninteracting bands. To do so we define a rotation matrix $M^{R,L}(\vec{k})_{n\sigma}$ such that $c_{\vec{k}n}^{L,R} = M^{L,R}(\vec{k})_{n\sigma} \psi_{\vec{k}\sigma}^{R,L}$. Note that the spin degeneracy is lifted and the noninteracting eigenstates are labeled by the band index $n = \pm$. The rotation matrices are unitary and rotate the spin quantization axis of each electron to point along its momentum \vec{k} .

We split the sum over momentum over \vec{k} for each $\psi_{\vec{k}, \sigma}$ into two, one with small momenta near the left node and the other with small momenta about the right node. An upper cutoff in energy, Λ , is imposed as the linear dispersion is a low-energy phenomena. Of the 16 possible terms from Eq. (2) only six terms satisfy momentum conservation for scattering restricted to the states within the cutoff around the node. For every momentum $\vec{q} = q\hat{q}$, where $\hat{q} = \{\hat{q}_x, \hat{q}_y, \hat{q}_z\}$ is the unit vector along \vec{q} , we define two orthogonal vectors $\hat{e}_{\vec{q}}^1 \equiv$

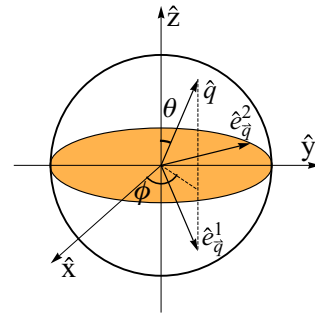


FIG. 1. (Color online) The interaction shown in Eq. (3) is a function of three vectors (\hat{q} , $\hat{e}_{\vec{q}}^1$, and $\hat{e}_{\vec{q}}^2$) that form a right-handed coordinate system. Each vector couples to an operator of distinct symmetry in the particle-hole channel.

$\hat{\theta}_{\vec{q}} = \{\hat{q}_x \hat{q}_z / \sqrt{\hat{q}_x^2 + \hat{q}_y^2}, \hat{q}_y \hat{q}_z / \sqrt{\hat{q}_x^2 + \hat{q}_y^2}, -\sqrt{\hat{q}_x^2 + \hat{q}_y^2}\}$ and $\hat{e}_{\vec{q}}^2 \equiv \hat{\phi}_{\vec{q}} = \{-\hat{q}_y / \sqrt{\hat{q}_x^2 + \hat{q}_y^2}, \hat{q}_x / \sqrt{\hat{q}_x^2 + \hat{q}_y^2}, 0\}$, such that \hat{q} , $\hat{e}_{\vec{q}}^1$ and $\hat{e}_{\vec{q}}^2$ form a right-handed coordinate system (see Fig. 1). The unit sphere is spanned by the vector \hat{q} by two rotations, one about any axis perpendicular to $\hat{e}_{\vec{q}}^2$ and the another about $\hat{e}_{\vec{q}}^2$. For example if we choose the first to be the z axis, then the vector $\hat{e}_{\vec{q}}^2$, which is the $\hat{\phi}$ in the spherical polar system, spans a unit circle (perimeter of the shaded region in Fig. 1) and the vector $\hat{e}_{\vec{q}}^1$, which is the corresponding $\hat{\theta}$, spans the southern hemisphere. The construction above holds for an arbitrary quantization axis \hat{n} , with the corresponding polar and azimuthal angle for \vec{q} defined in the coordinate frame $\{\hat{l}, \hat{m}, \hat{n}\}$. In the rest of the paper we use the $\{\hat{x}, \hat{y}, \hat{z}\}$ coordinate system. The particular choice of the coordinate system breaks spatial rotational invariance.

Specializing to potentials that are even functions of \vec{k} , i.e., $V(\vec{k}) = V(-\vec{k})$, the interaction is

$$V_c = \sum_{\vec{k}, \vec{k}', \tau, n} \left[\frac{V(\vec{k} - \vec{k}') - V(\vec{k} + \vec{k}') - 2\tau \vec{K}_0}{2} \times (\hat{e}_{\vec{k}}^1 \cdot \hat{e}_{\vec{k}'}^1 + \hat{e}_{\vec{k}}^2 \cdot \hat{e}_{\vec{k}'}^2) (c_{\vec{k}n}^{\tau\dagger} c_{-\vec{k}n}^{-\tau\dagger} c_{-\vec{k}'n}^{-\tau} c_{\vec{k}'n}^{\tau}) + \frac{V(\vec{k} - \vec{k}')}{2} (1 + \hat{k} \cdot \hat{k}') c_{\vec{k}n}^{\tau\dagger} c_{-\vec{k}n}^{\tau\dagger} c_{-\vec{k}'n}^{\tau} c_{\vec{k}'n}^{\tau} \right]. \quad (3)$$

$\tau = \pm$ refer to the two (left and right) nodes. We have dropped terms of the form $c_{\vec{n}\vec{k}}^{\tau_1\dagger} c_{-\vec{n}-\vec{k}}^{\tau_2\dagger} c_{-\vec{n}-\vec{k}'}^{\tau_2} c_{\vec{n}\vec{k}'}^{\tau_1}$ and $c_{\vec{n}\vec{k}}^{\tau_1\dagger} c_{\vec{n}-\vec{k}}^{\tau_2\dagger} c_{-\vec{n}\vec{k}}^{\tau_2} c_{-\vec{n}-\vec{k}'}^{\tau_1}$ which lead to pairing of states which are not degenerate in the noninteracting limit. For attractive interaction we get the very rich structure, with a number of possible superconducting phases. The first two terms in Eq. (3) lead to internodal pairing, which gives the zero momentum BCS¹⁶ state, while the last term, the intranodal pairing term, yields finite momentum pairing states (FFLO^{14,15}). In the rest of the paper we analyze the instabilities within mean field.

III. MEAN-FIELD ANALYSIS

A. Local interactions

For local interactions the BCS channel vanishes. To understand why, note that the interaction is one where we destroy

particles at \vec{k} and $-\vec{k}$ and create them at \vec{k}' and $-\vec{k}'$. Thus there are two possibilities: put the first particle at \vec{k}' and the second at $-\vec{k}'$ or vice versa. These are inequivalent processes, as evident from the different momentum transfer involved, among indistinguishable particles. The exchange produces a relative minus sign. For local interaction the weight of both the processes are identical leading to an exact cancellation. Note that this result is very different from that of the model with lower symmetry such as the C_{4h} symmetric model studied by Cho *et al.*,¹¹ where the BCS channel is also unstable for local attraction. The reason for the difference arises from the fact that in our model the spins at \vec{k} and $-\vec{k}$ are parallel for all \vec{k} . Thus the two processes only pick up a relative sign independent of the spin orientation. For the C_{4h} symmetric models, whether the particle at \vec{k} ends up at \vec{k}' or $-\vec{k}'$ also determines a relative factor that accounts for the different spin orientation of the two final states. This mitigates the cancellation for all momenta. Nevertheless, in both cases the finite momentum pairing wins out. Tipping the system to favor the BCS state requires fine tuning.

In the finite momentum pairing channel, there are two equally attractive channels corresponding to order parameters of the form $\Delta_s = \langle \sum_{\vec{k}} c_{-\vec{k}n}^\tau c_{\vec{k}n}^\tau \rangle$ and $\Delta_p = \langle \sum_{\vec{k}} \hat{k} c_{-\vec{k}n}^\tau c_{\vec{k}n}^\tau \rangle$. The former is the even-parity (s -wave) while the latter is odd-parity (p -wave) superconductor. Note that the anticommutation of fermionic operators implies that $\Delta_s = 0$. This is expected as nondegenerate states cannot pair in the singlet channel and only odd orbital pairing survives. For local attractive interaction, $V(\vec{k}) = g/\Omega$ where g is a constant and Ω is the volume of the system. Following similar standard mean-field analysis in Ref. 8, the gap equation for the p -wave channel at zero temperature is

$$1 = \frac{g}{2} \sum_{\vec{k}} \frac{|\hat{\Delta}_p \cdot \hat{k}|^2}{\sqrt{(\hbar v k)^2 + |\hat{\Delta}_p \cdot \hat{k}|^2}}. \quad (4)$$

In general the complex order parameter takes the form $\vec{d}_1 + i\vec{d}_2$ and extremization yields two possible structures: (i) $\vec{d}_1 \cdot \vec{d}_2 = 0$, $|\vec{d}_1| = |\vec{d}_2|$ and (ii) $\vec{d}_1 || \vec{d}_2$, $\vec{d}_1 + i\vec{d}_2 = \vec{d} e^{i\phi}$ where \vec{d} is a real vector.¹⁷ Minimization of the gap equation for the two cases yields the axial vacuum [case (i)] as the ground state and thus a chiral superconductor is stabilized. This state has nodes in the gap, with linearly dispersing massless charged excitations, in complete analogy with the A phase of superfluid ^3He . Equation (4) is identical to the gap equation obtained for the excitonic phases for repulsive interaction.⁸ Reading off the results we note that a minimum interaction strength of $g_c = 3(\hbar v)^3/2\pi\Gamma^2$ is required for the state to be realized for chemical potential at the node. Here $\Gamma < \Lambda$ is the cutoff in energy of the attractive interaction. At the mean-field level, the CDW instability is also possible for attractive interaction.^{8,9} The critical coupling is smaller as compared to the superconducting state and opens a full gap (i.e., no nodes). Thus the nodal finite momentum superconducting state is always disfavored as compared to the CDW.

At finite chemical potential the particle-hole nesting between the nodes is lost and only the superconducting state is realized. Moreover, for finite chemical potential μ , the state is precipitated for infinitesimal interaction strength.

For $\mu - \Gamma > 0$ and $\mu + \Gamma < \Lambda$, the attractive interaction is operative only for the positive energy sector of the theory with linear dispersion. For this case the transition temperature is $2K_B T_c \approx \Gamma \exp[-3/gv(\mu)]$ where $\nu(\mu) = \mu^2/2\pi^2(\hbar v)^3$ is the density of states at the chemical potential.

B. Nonlocal interactions

For local interaction $V(\vec{k} - \vec{k}') = V(\vec{k} + \vec{k}' - 2\tau\vec{K}_0)$ and no internodal pairing is allowed. For nonlocal interaction, the cancellation does not occur and a BCS state can precipitate. This state competes with the p -wave intranodal pairing state. Which of the two wins depends on the details of the interaction. To identify the possible phases, we assume an attractive interaction of the form

$$V(\vec{k}) = \begin{cases} -g & \text{if } |\vec{k}| < |\vec{K}| < |\vec{K}_0|, \\ 0 & \text{otherwise} \end{cases} \quad (5)$$

for some fixed \vec{K} . Thus the attraction has a range of order $1/|\vec{K}|$ smaller than $1/|\vec{K}_0|$. While this simplifies the algebra, the symmetry arguments below hold in general. Let us now consider the two attractive channels: (1) $\bar{\Delta}_1 = \langle \sum_{\vec{k}} \hat{e}_k^1 c_{-\vec{k}n}^\tau c_{\vec{k}n}^\tau \rangle$ and (2) $\bar{\Delta}_2 = \langle \sum_{\vec{k}} \hat{e}_k^2 c_{-\vec{k}n}^\tau c_{\vec{k}n}^\tau \rangle$. Since \hat{e}_k^1 is even under inversion, i.e., $\hat{e}_k^1 = \hat{e}_{-\vec{k}}^1$, $\bar{\Delta}_1 = 0$. This is analogous to the even orbital parity channel vanishing in the intranodal case.

There are two possible superconducting states for $\bar{\Delta}_2$: (1) $\bar{\Delta}_2 = \langle \sum_{\vec{k}} \hat{e}_k^2 c_{-\vec{k}n}^\tau c_{\vec{k}n}^\tau \rangle = \Delta_{2p} \hat{x}$ and (2) $\bar{\Delta}_2 = \langle \sum_{\vec{k}} \hat{e}_k^2 c_{-\vec{k}n}^\tau c_{\vec{k}n}^\tau \rangle = \Delta_{2c} (\hat{x} + i\hat{y})/\sqrt{2}$. The p and c labels refer to polar and chiral respectively. The structure of the order parameters is dictated by symmetry. Once the spatial rotational symmetry is broken by a choice for the quantization axis, the vector \hat{e}_2 lies in the plane perpendicular to it. As the vector \hat{k} sweeps out the unit sphere, \hat{e}_2 spans a unit circle in this plane (see Fig. 1). Thus the order parameter in this case is either a polar vector in the plane (chosen to be \hat{x} for illustrative purposes) or chiral. Within mean field, the spectrum for the quasiparticles for the two cases are $E_{2p} = \sqrt{(\hbar v k)^2 + |\Delta_{2p}|^2} \cos^2 \phi$ and $E_{2c} = \sqrt{(\hbar v k)^2 + |\Delta_{2c}|^2}$, where ϕ is the azimuthal angle in the $\{\hat{x}, \hat{y}, \hat{z}\}$ coordinate system. The polar state has line nodes while the chiral state is gapped. On minimization of the free energy, the latter is energetically favored. It is also more favorable as compared to the finite momentum pairing state.

For chemical potential at the node a minimum coupling strength of $g_c = (\hbar v)^3/2\pi\Gamma^2$ is needed to nucleate this state. Here $\Gamma = \hbar v|\vec{K}|$ is the energy corresponding to the cut off in momentum in Eq. (5). Since the intranodal pairing depends only on the small wavelength part of the interaction, the instability criterion is the same for the interaction in Eq. (5) as the short-range interaction. The critical coupling is three times larger in the latter case, so that for nonlocal interactions the chiral BCS state is the preferred ground state.

For finite chemical potential, the transition temperature for the chiral BCS state is $2K_B T_c \approx \Gamma \exp[-1/2gv(\mu)]$. Thus the transition temperature is higher than that of the finite pairing state given by $2K_B T_c \approx \Gamma \exp[-3/gv(\mu)]$. The difference arises from the angular dependence of the gap in the finite momentum state which has nodes at the poles.

IV. TOPOLOGICAL EXCITATIONS AND EFFECT OF DISORDER

For local interactions the lowest energy state is the finite momentum pairing in the odd-parity channel. Such a state has nodes at the north and south pole of the spherical Fermi surface. In complete analogy with the corresponding states for spinless version of the equal spin pairing states in ^3He ,¹⁷ they support relativistic massless Fermionic excitations. The existence of these nodal points leads to surface states at zero energy. As discussed in Refs. 11 and 18 the vortex of finite momentum pairing state is made up of two half quantum vortices, where the phase only winds around one of the Weyl nodes but not the other. The fact that Fermi surface encloses a Berry phase of π implies that each half vortex hosts a Majorana mode at its core. In general the hybridization between the two will gap them out as they are not protected by any symmetry. For nonlocal interaction, the odd-parity BCS state wins out. This state is fully gapped.

It is known that spin-orbit interaction leads to suppression of the deleterious effects of disorder induced pair breaking on superconductivity.¹⁹ In particular scalar disorder cannot mix states with different chirality. Stated differently scattering between different spin-momentum locked states acquire angular dependencies arising from mismatch in spin orientation. The nontrivial dependence leads to vanishing dephasing rate yielding robust superconductivity.¹⁹

V. CONCLUSION

In this section we compare and contrast our work to those in the literature. To understand why only odd pairing superconductivity is obtained, it is important to note that the bands that touch are spin nondegenerate. In other words, in the low-energy effective theory there are two states per momentum which are split in energy. Chirality is a good quantum number but not spin. Given this, it is not possible to form spin singlets among degenerate states, as only one of the two “spin” states is available. Previous studies on the interplay of spin orbit and superconductivity^{10,11} perform the mean-field decomposition

before projecting to the chiral basis. In other words a projection to singlet states is made before accounting for the splitting due to spin orbit. This allows for finite pairing amplitude among states that are nondegenerate in energy in the noninteracting limit (i.e., mixes the valence and conduction bands). For chemical potential at the node these yield a class of even-parity superconducting states for the C_{4h} symmetric models. They are absent in the Weyl semimetals studied here.

Another important distinction is that in the minimal model assumed here of two Weyl nodes, the Pauli matrices represent spin. In particular they do not change under inversion. In a certain class of effective theories, the inversion operator takes the form $I : \sigma^z H(-k) \sigma^z$.^{3,11} In this case the sign of the spin operators for the transverse directions changes under inversion. This additional symmetry leads to a set of superconducting states that allow for even-parity spin singlet pairing. The reason is that the spin state at \vec{k} and $-\vec{k}$ are no longer the same, as one would expect if inversion was an identity operator on spins. Thus there is a finite projection of singlet states onto the spin texture in the chiral basis.

A final point to note is that a full lattice model (as opposed to the low-energy effective theory considered here) has linear dispersion for a finite-energy window around the node. Thus any analysis that uses the full energy dispersion includes the deviation from linearity. This is especially true for doped systems with large chemical potentials. Nevertheless the nondegeneracy of the bands and the spin structure allow for odd-parity superconductors. Whether the even- or odd-parity states win out in this case is deferred to future investigations.

In summary, Weyl semimetals are shown to display robust odd-parity superconductivity, with both zero and finite momentum Cooper pairs.

ACKNOWLEDGMENTS

The authors thank C. Varma for helpful discussion and comments. H. Wei and V. Aji acknowledge the financial support by University of California at Riverside through the initial complement. S. P. Chao acknowledges financial support by NCTS in Taiwan.

¹C. Herring, *Phys. Rev.* **52**, 365 (1937).

²X. Wan, A. M. Turner, A. Vishwanath, and S. Y. Savrasov, *Phys. Rev. B* **83**, 205101 (2011).

³A. A. Burkov and L. Balents, *Phys. Rev. Lett.* **107**, 127205 (2011).

⁴P. Hosur, S. A. Parameswaran, and A. Vishwanath, *Phys. Rev. Lett.* **108**, 046602 (2012).

⁵V. Aji, *Phys. Rev. B* **85**, 241101 (2012).

⁶A. A. Zyuzin and A. A. Burkov, *Phys. Rev. B* **86**, 115133 (2012).

⁷P. Goswami and S. Tewari, *Phys. Rev. B* **88**, 245107 (2013).

⁸H. Wei, S.-Po Chao, and V. Aji, *Phys. Rev. Lett.* **109**, 196403 (2012).

⁹Z. Wang and S. C. Zhang, *Phys. Rev. B* **87**, 161107(R) (2013).

¹⁰T. Meng and L. Balents, *Phys. Rev. B* **86**, 054504 (2012).

¹¹G. Young Cho, J. H. Bardarson, Y.-M. Lu, and J. E. Moore, *Phys. Rev. B* **86**, 214514 (2012).

¹²Y. Li and C. Wu, *Sci. Rep.* **2**, 392 (2012).

¹³J. D. Sau and S. Tewari, *Phys. Rev. B* **86**, 104509 (2012).

¹⁴P. Fulde and R. A. Ferrell, *Phys. Rev.* **135**, A550 (1964).

¹⁵A. I. Larkin and Yu. N. Ovchinnikov, *Sov. Phys. JETP* **20**, 762 (1965).

¹⁶J. Bardeen, L. N. Cooper, and J. R. Schrieffer, *Phys. Rev.* **106**, 162 (1957).

¹⁷G. Volovik, *Universe in a Helium Droplet* (Oxford University Press, New York, 2003).

¹⁸O. Dimitrova and M. V. Feigel'man, *Phys. Rev. B* **76**, 014522 (2007).

¹⁹K. Michaeli and L. Fu, *Phys. Rev. Lett.* **109**, 187003 (2012).